Electronic Supplementary Material (ESI) for Journal of Materials Chemistry C.

Supplementary Information

$La_{0.4}Gd_{1.6}Zr_2O_7$:0.1%Pr transparent sintered ceramic - a wide-range luminescence thermometer

Joanna Trojan-Piegza[1,*,‡], Carlos D. S. Brites[2, ‡], João F. C. B. Ramalho[2], Zhengjuan Wang[3], Guohong Zhou[3], Shiwei Wang[3], Luís D. Carlos[2,1] and Eugeniusz Zych[1,2]

[1]Faculty of Chemistry, University of Wroclaw, 14. F. Joliot-Curie Street, 50-383 Wroclaw, Poland

[2]Phantom-g, CICECO-Aveiro Institute of Materials, Physics Department, University of Aveiro, 3810-193 Aveiro, Portugal

[3]The State Key Lab of High Performance Ceramics and Superfine Microstructure, Shanghai Institute of Ceramics, Chinese Academy of Sciences, Shanghai 200050, China

S1. *Material morphology*

The microstructure of the investigated LGZO:0.1%Pr transparent ceramic is presented in Figure S1 upon two different magnifications: 500x (top) and 2000x (bottom). Very efficient densification is proved and no voids or pores can be seen within the material body. This results in a very low loss of in-line transmittance as presented in Figure S2. The material was sintered at 1850 °C.[1] Hence, there is no fear that its microstructure will undergo any changes at temperatures at which its thermometric properties are tested in this work.

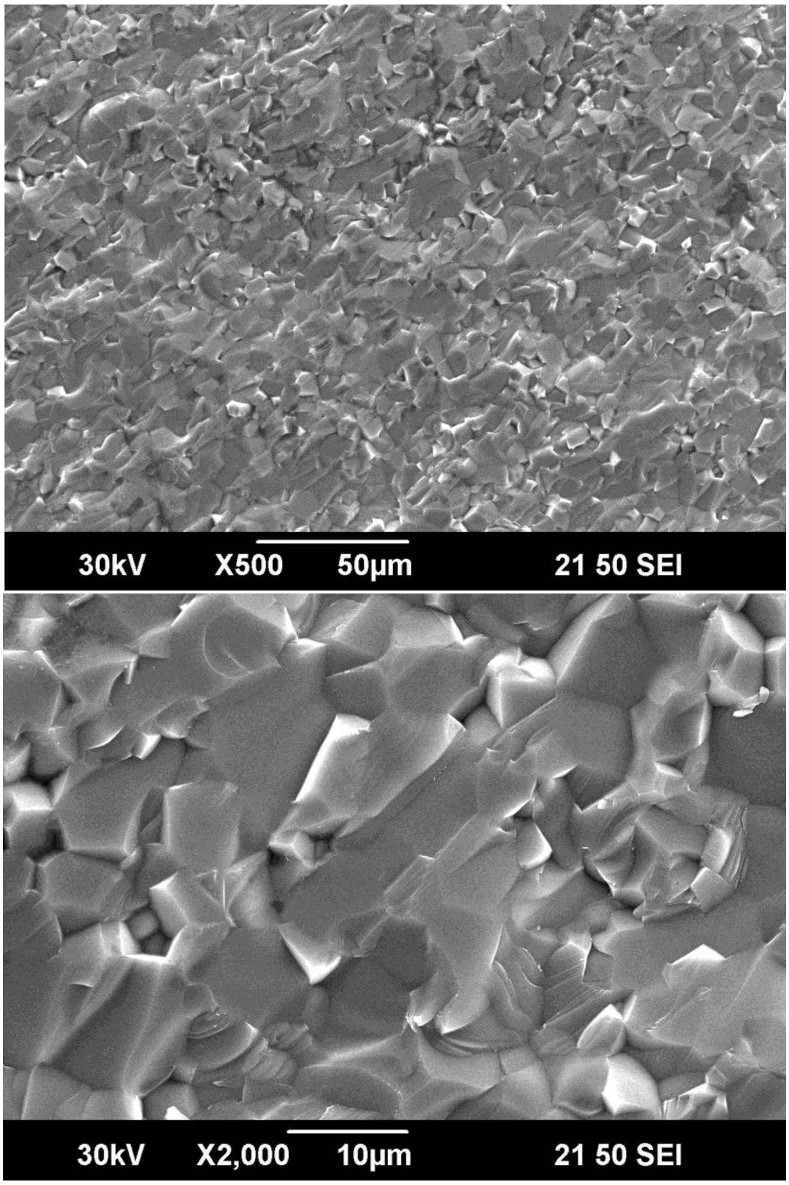

Figure S1. The microstructure of the $La_{0.4}Gd_{1.6}Zr_2O_7$*:0.1%Pr sintered ceramic upon different magnifications.*

S2. *Transmittance and absorption spectrum of the LGZO:0.1%Pr sintered ceramic*

Transmission and absorption spectra of the LGZO:0.1%Pr ceramic are presented in Figure S2. The transmittance of the ceramic reaches 72.5% at 633 nm and 74% at 1000 nm. These values reach 94.3 % of the highest theoretical transmittance of ideally transparent LGZO as discussed in [1]. The strong absorption below 350 nm is related to the 4f→5d allowed transition of Pr^{3+}. It will be seen in the excitation spectra of Pr^{3+} luminescence presented in Figure S3.

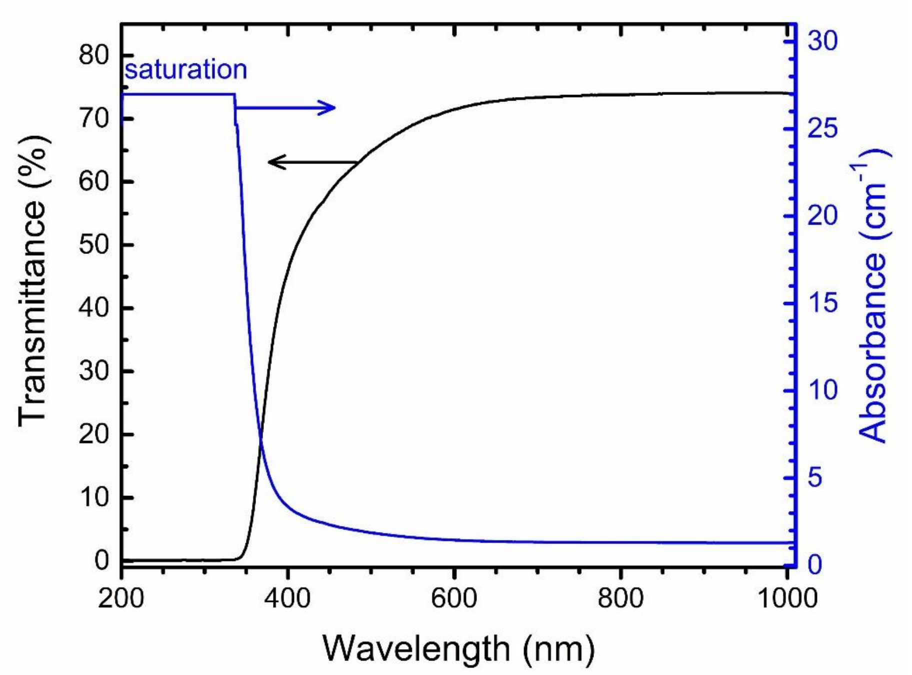

Fig. S2. Transmittance and absorption spectrum of the LGZO:0.1%Pr ceramic 1 mm thick.

S3. *Temperature dependence of LGZO:0.1%Pr excitation spectra*

Figure S3 presents excitation spectra of 608 nm Pr^{3+} luminescence. At this wavelength mainly the $^1D_2$ emission is observed but an admixture of transitions from the $^3P_0$ level is also present (compare Figure 2). The spectra were recorded at 15, 150, 300, and 600 K. In the UV part a broad band representing the 4f→5d transition and coinciding with the strong absorption of the material (see Figure S2) is present. At the lowest temperature, 15 K, a broad band peaking around 340 nm and partially overlapping with the 4f→5d band is seen. It is presumably related to a defect. From Figure S3 it is clear that the Pr^{3+} luminescence can be effectively excited either by the intra-configurational 4f→5d transition in UV or by the $^3H_4 \rightarrow {}^3P_J$ blue band (in 425-500 nm range). Choosing the latter poses a problem of effective separation of the excitation and emission especially at higher temperatures when the luminescence features become very broad (see Figure 3a). Therefore, we have chosen excitation into the UV 4f→5d band.

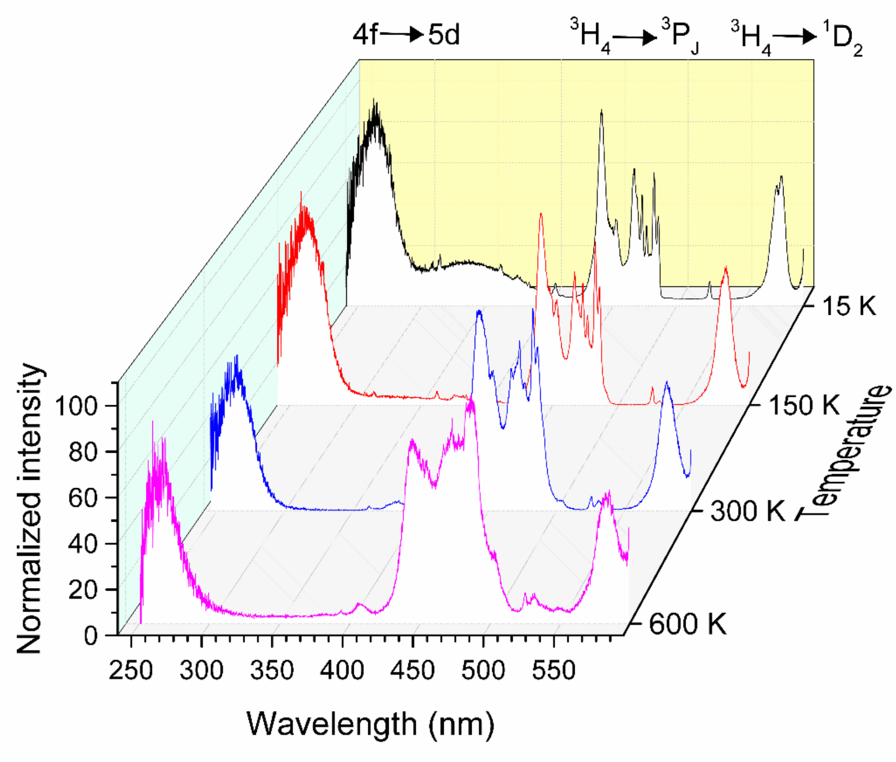

Figure S3. Excitation spectra of 608 nm luminescence (at which wavelength both emission from $^3P_0$ and $^1D_2$ is seen) recorded at indicated temperatures. A the lowest temperature (15 K) a defect related feature around 350 nm appears.

S4. ***Temperature dependence of decay kinetics of $^3P_0$ and $^1D_2$ luminescence***

Figure S4 presents temperature dependence of kinetics of the two emission of Pr^{3+}. Decay curves of the $^3P_0$ luminescence are seen in Figure S4a and those of $^1D_2$ emission in Figure S4b. Both figures show also the relative instrumental response functions (IRF, red points), which exposes the temporal evolution of the excitation pulse. This proves that the spikes at the beginning of the traces are related to the excitation pulses of the Xe-lamp not to any very short components. All traces only slightly deviated from the single exponential dependence. Nevertheless, good fits needed using a two-exponential dependence according to Eq. S1:

$$I = A_1 \exp\left(-\frac{t}{\tau_1}\right) + A_2 \exp\left(-\frac{t}{\tau_2}\right) + A_0, \qquad \text{(S1)}$$

where I is the intensity at time t, τ_1 *and* τ_2 are the decay time constants, A_1 and A_2 are fitting constants and A_0 is a background signal. The temperature dependence of the derived time constants of both emissions is presented in Figure S4c. The luminescence from the $^3P_0$ level is by a factor of ~15 shorter (at 15 K) than emission from the $^1D_2$. This is a typical difference since transitions from $^3P_0$ are spin-allowed whilst from $^1D_2$ are spin- and parity-forbidden.[2] The decay times of the two emissions (Figure S4c) shorten with temperature indicating thermally stimulated nonradiative draining of the emitting levels, as discussed in the main paper. As anticipated, however, the luminescence of $^1D_2$ shows the first sign of thermal quenching at 250 K, while the decay of the $^3P_0$ emission shortens slightly right above 15 K and above 150 K the quenching becomes significant. Clearly, $^3P_0$ level is more susceptible to thermal quenching, as explained in the main paper.

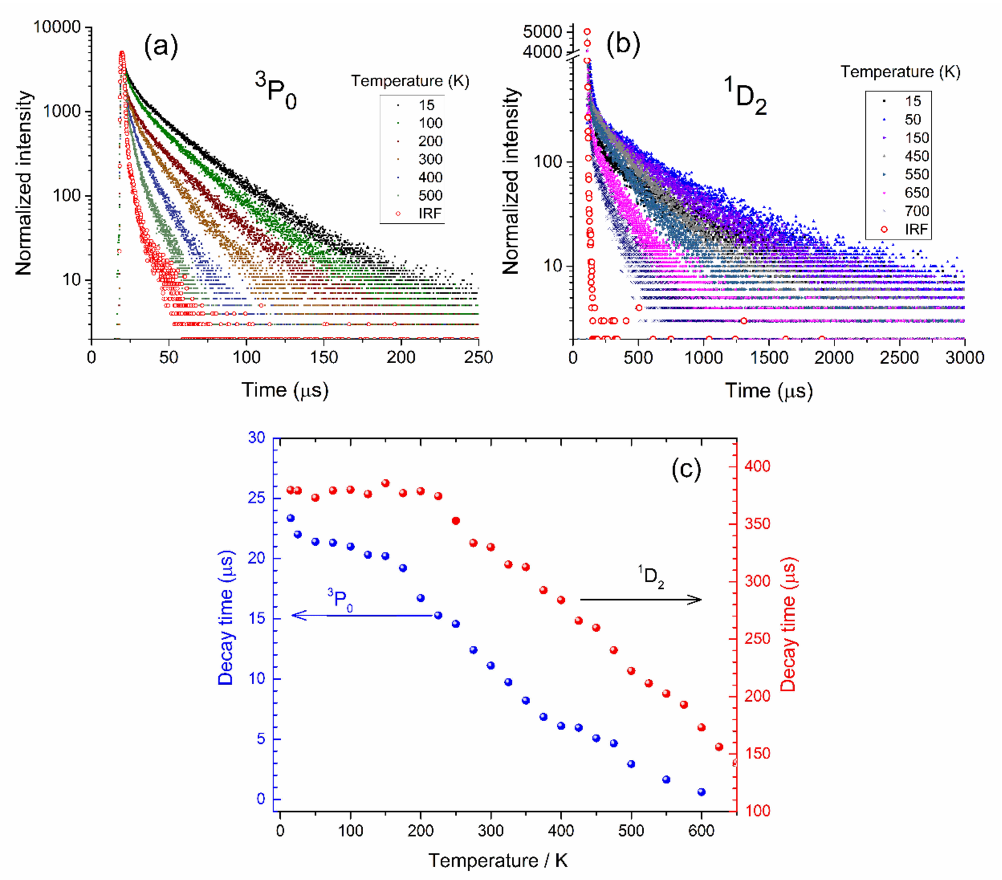

Figure S4. Decay curves of the $^3P_0$ (a), and $^1D_2$ emissions at selected temperatures. Temperature-dependence of decay times derived from the curves for both emissions (c). IRF stands for instrumental response function presenting a temporal evolution of the excitation signal.

S5. *References*

1 Z. Wang, G. Zhou, X. Qin, Y. Yang, G. Zhang, Y. Menke and S. Wang, *J. Alloys Compd.*, 2014, **585**, 497–502.

2 G. Blasse and B. C. Grabmaier, *Luminescent Materials*, Springer-Verlag, Berlin Heidelberg, 1994.